

External Modulation of Rayleigh-Bénard Convection

Joseph J. Niemela and Russell J. Donnelly

Department of Physics, University of Oregon, Eugene, Oregon 97403

(Received 7 August 1987)

We report thermal-convection experiments using helium I where the vertical temperature difference has an externally imposed time dependence. Both positive and negative threshold shifts are observed depending on the strength and rate of modulation, as well as a depression of the initial slope of the heat transfer above threshold, in qualitative agreement with predictions of Ahlers, Hohenberg, and Lücke and of Rosenblat and Herbert.

PACS numbers: 47.20.Bp, 44.25.+f, 47.25.Qv

There has been a growing interest recently in externally modulated hydrodynamic systems, both theoretically¹⁻⁷ and experimentally.⁸⁻¹² These systems may exhibit novel behavior in response to parametric forcing near a point of instability. Many other nonlinear physical systems, including those of a mechanical or electrical nature, likewise exhibit altered behavior when external parameters are varied appropriately.¹³ An example from hydrodynamics is thermal convection between two horizontal boundaries, where the driving force has an imposed time dependence due to temporal modulation of the boundary temperatures. Depending on the relative strength and rate of the forcing, predictions exist for a variety of responses to the modulation. Among these are the upward shift of the convective threshold compared to the unmodulated problem¹⁻⁷ (reminiscent of the enhanced stability characteristics of the classical inverted pendulum¹⁴), as well as changes in the nonlinear heat transport above threshold⁴ and in the nature of the bifurcation of the transition.³⁻⁶ Although there has been much theoretical interest in this problem there is little experimental data^{8,10,11} available for comparison.

We report thermal-convection experiments involving temporal variation of the temperature difference across a layer of fluid contained in a cryogenic Rayleigh-Bénard cell of cylindrical geometry. Helium I was used as the working fluid at an operating temperature of 2.63 K and a Prandtl number $\sigma=0.49$, where $\sigma=\nu/\kappa$ and ν, κ are respectively the kinematic viscosity and thermal diffusivity of the fluid. Our cell has a height $d=0.0917$ cm and a radius-to-height ratio of 8.82, with upper and lower plates made of oxygen-free high-conductivity copper and separated by a thin (0.015-cm thickness) cylindrical stainless-steel wall. Two matched germanium resistance thermometers embedded in the top and bottom plates and configured as one arm of an ac bridge measure the temperature difference ΔT produced by supplying heat to the bottom plate by means of the off-balance bridge voltage. The driving force for convection is represented by the Rayleigh number $N_{Ra}=ga\Delta Td^3/\nu\kappa$, where g is the acceleration of gravity, and ΔT is the temperature difference across the layer of fluid of height d and isobaric thermal expansion coefficient α . In addition,

the horizontally averaged heat transport across the fluid is characterized by the Nusselt number N_{Nu} , defined as the ratio of the measured effective thermal conductance of the fluid to its value in the absence of motion (molecular heat transport only), so that $N_{Nu} > 1$ implies convection.

A recent theoretical treatment of externally modulated Rayleigh-Bénard convection has been undertaken by Ahlers, Hohenberg, and Lücke⁴ (AHL) on the basis of a mode truncation of the Oberbeck-Boussinesq hydrodynamic equations, i.e., on a generalized version of the Lorenz model,¹⁵ keeping only the lowest spatial Fourier modes for the convective velocity and temperature, which here will be represented by $x(t)$ and $y(t)$, respectively. A second convective temperature mode $z(t)$ represents a spatial average of the temperature in the horizontal plane, depending only on the vertical coordinate, and is related to the Nusselt number. Using the notation of AHL, for a sinusoidal modulation of the temperature difference across the cell $\Delta T(t)=\Delta T[1+\Delta\cos(\omega t)]$ we write the time-dependent *relative* Rayleigh number for a Boussinesq fluid as $r(t)=r_0+\delta\cos(\omega t)$, where the Rayleigh number has been normalized by its critical value in the absence of modulation $N_{Ra,c}^{stat}$. ΔT and r_0 are time-averaged quantities given by $\Delta T=\langle\Delta T(t)\rangle$ and $r_0=\langle N_{Ra}(t)\rangle/N_{Ra,c}^{stat}$, where the angular brackets signify averaging over time, and $\delta=r_0|\Delta|$. Times are nondimensionalized by the vertical thermal diffusion time d^2/κ , so that, e.g., $\omega=\omega^*d^2/\kappa$, where ω^* has dimensions of radians per second. Because oscillating temperatures at the boundaries give rise to "heat waves," which distort the conduction temperature profile in the fluid from one which is simply linear in space, $r(t)$ is modified by the introduction of a new parameter $\delta'=r_0|\Delta'(\omega)|$, with $\Delta'(\omega)$ being a frequency-dependent amplitude defined by AHL (with a correction¹⁶). The Lorenz model appropriate to rigid horizontal boundaries is then given by AHL:

$$\tau_1 dx/dt = -\sigma'[x(t) - y(t)], \quad (1a)$$

$$\tau_1 dy/dt = -y(t) + [r'(t) - z(t)]x(t), \quad (1b)$$

$$\tau_1 dz/dt = -b[z(t) - x(t)y(t)]. \quad (1c)$$

Here, $b=2$, $\tau_1=(2\pi^2)^{-1}$, $\sigma'=27\sigma/14$, and $r'(t)$ is just $r(t)$ with δ replaced by δ' .

Equations (1) describe a laterally infinite layer of fluid and predict positive threshold shifts which approach a maximum as $\omega \rightarrow 0$. To describe modulated convection in a finite container, inhomogeneous forcing terms are added to Eqs. (1), making the bifurcation imperfect. In this case, as discussed by AHL, the threshold for convection is no longer uniquely defined; however, it is possible to define an effective threshold as, say, the value of $\epsilon = N_{Ra}/N_{Ra,c}^{\text{stat}} - 1$ for which the average amplitude of the convective temperature mode $\langle z(t) \rangle$ exceeds 0.001.

The inhomogeneous term is added to Eq. (1a) which then reads

$$\tau_1 dx/dt = -\sigma'[x(t) - y(t)] + \sigma'\xi(t), \quad (1a')$$

where $\xi(t)$ is the forcing term given in Eq. (D15) by AHL. In terms of the various modulation parameters $\xi(t)$ can be written as

$$\xi(t) = f\omega\delta[\text{Im}\psi(\omega)\cos(\omega t) - \text{Re}\psi(\omega)\sin(\omega t)],$$

where $\psi(\omega)$ is defined in their Eq. (D18) and behaves like $|\psi(\omega)| \rightarrow 1$, $\psi = \psi(\text{real})$ as $\omega \rightarrow 0$ and $|\psi(\omega)| \rightarrow 0$ as $\omega \rightarrow \infty$, and the forcing strength f is taken to be an adjustable constant which is fitted to the experiment. At low frequencies of modulation the forcing induces strong convective motions at values of r_0 below the threshold predicted by the homogeneous equations.

In a different way, Rosenblat and Herbert¹ (RH) also find apparent destabilization at low frequencies through an amplitude criterion when the horizontal boundaries are stress-free. Such a criterion is motivated by consideration of the validity of a linear stability analysis at low frequencies, where disturbance amplitudes may have time to grow to sufficiently large values during the unstable portion of the modulation cycle that nonlinear effects become significant. By this criterion, flows are considered stable if the amplitude of the least stable disturbance mode grows no more than a factor of m times some initial value over a complete cycle, corresponding to a value of $M = \log(m)$ which RH take to be of order 1, but otherwise arbitrary. The envelope of the amplitude-criterion results, assumed to be valid at low frequencies, with thresholds predicted by standard linear stability theories [e.g., the homogeneous Eqs. (1) appropriate for free boundaries], which should be valid at higher frequencies, produces a finite optimum frequency for which the stabilization is maximum (rather than the limiting value $\omega \rightarrow 0$). As noted by RH, this is in qualitative agreement with the threshold behavior of the analogous Couette-Taylor experiments of Donnelly.¹⁷ RH found broad agreement with the Couette results by choosing $M=2.25$, and we note that for Δ of order unity and $\sigma=0.49$, this choice of M predicts an optimum frequency of $\omega \approx 7$, which compares well with our observation of an optimum frequency near $\omega=10$, for $\Delta \sim 1$.

Two different methods of producing time-varying temperatures were used for this experiment. For low frequencies, the method used in previous studies^{8,10} of sinusoidally heating the bottom plate proved adequate. Here, a modulated heating current $Q(t) = Q_0[1 + \Delta_Q \times \cos(\omega t)]$ is applied to the lower plate while the upper plate has its temperature controlled to be constant. If we take into account the finite heat capacities of the lower plate and fluid for our cell, as well as the fact that cooling can only be accomplished by conduction through the fluid and side walls, the temperature amplitude yielded for such a modulation decreases monotonically with frequency from a maximum of $\Delta=1$ at $\omega=0$ to less than $\Delta=0.2$ for $\omega \sim 10$. To obtain large amplitudes at higher frequencies, then, it is necessary to employ a novel technique which involved heating *and cooling* the top plate of our cell, which is in contact with a colder superfluid helium bath. Specifically, the modulation is accomplished by our superimposing a time-varying electrical current on the output of a feedback circuit used to regulate the top-plate temperature, so that the temperature can be made to oscillate about a controlled mean (see Ref. 11). To obtain a nonzero mean temperature difference across the cell, a steady heat Q is applied to the bottom plate simultaneously with the top-plate modulation, where the oscillation amplitude of the top-plate temperature can be made to increase linearly with Q , thus fixing Δ in the conductive regime. A waiting time is then initiated before we collect data to allow the system to adjust to the modulation; e.g., at $\omega \sim 10$ this time was typically 25–30 modulation cycles, corresponding to 15–20 characteristic vertical thermal diffusion times of the fluid. The attainment of steady-state conditions is easily confirmed by our monitoring $\Delta T(t)$ on an external recording device.

The results from a modulation run are interpreted in much the same manner as for standard convection, i.e., by our first converting the measured data $\langle Q(t) \rangle$, $\langle \Delta T(t) \rangle$ into Nusselt-number and Rayleigh-number pairs and then plotting $N_{Nu} - 1$ vs ϵ , where $\epsilon = N_{Ra}/N_{Ra,c}^{\text{stat}} - 1$ and N_{Nu} and N_{Ra} are to be understood to be averages over a modulation cycle. We determine the critical value of the Rayleigh number by making a linear least-squares fit of lines to the data above ($N_{Nu} > 1$) and below ($N_{Nu} = 1$) threshold and finding their point of intersection, excluding from the fit the “rounded” points in the immediate vicinity of the onset, as well as those points in the “saturated” region well above onset where the heat-transfer slope shows negative curvature.

Figure 1 shows data obtained for low frequencies, with use of mainly bottom-plate modulation with fixed $\Delta_Q = 0.98$, where $0.5 < \Delta < 1$. It is clear that the stabilization predicted by the homogeneous Eqs. (1) for the ideal layer is not realized experimentally, with apparent destabilization of up to 40%. On the other hand, for comparable amplitudes and higher frequencies, which required top-plate modulation, this stabilization is readily

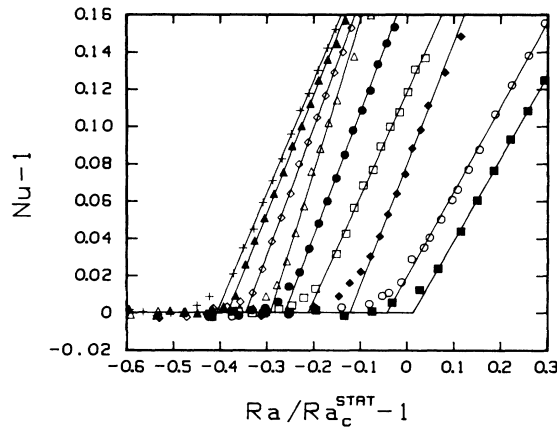


FIG. 1. Low-frequency modulation. Values of the frequency ω and amplitude Δ are as follows: crosses, $\omega=0.222$, $\Delta=0.98$; filled triangles, $\omega=0.444$, $\Delta=0.92$; open lozenges, $\omega=0.667$, $\Delta=0.90$; open triangles, $\omega=0.889$, $\Delta=0.81$; filled circles, $\omega=1.11$, $\Delta=0.75$; open squares, $\omega=1.33$, $\Delta=0.69$; filled lozenges, $\omega=1.78$, $\Delta=0.58$; open circles, $\omega=3.33$, $\Delta=0.68$; filled squares, $\omega=4.44$, $\Delta=0.68$. The solid lines are linear least-squares fits to the data above and below the convective threshold.

apparent as seen in Fig. 2(a), where we present data for $\omega=10.7$. In Fig. 2(b), these data are compared to predictions for the ideal layer, where the convective thresholds are plotted against $\delta'_c = (1 + \epsilon_c) |\Delta'(\omega)|$. Also shown (dashed line) are the effective thresholds $\epsilon_c = \epsilon_c^{\text{eff}} [\langle z(t) \rangle = 0.001]$ resulting from integrating Eqs. (1) with the inhomogeneous forcing term and a forcing strength $f=0.0004$. Specifically, an integrating step size $\Delta t < \min(0.02, \pi/16\omega)$ was used with initial values $x=y=z=0$. In all integrations, $z(t)$ was monitored graphically to verify the attainment of steady conditions.

It is clear from Fig. 2(b) that the predictions for the ideal layer, and the effective threshold behavior resulting from inclusion of the inhomogeneous forcing term in Eqs. (1), are very close to one another for a forcing strength $f=0.0004$. For lower-frequency modulation, however, the effective thresholds predicted for this forcing, as well as the experimental results, differ substantially from the ideal behavior, which predicts increasing stabilization as $\omega \rightarrow 0$. This is evident in Fig. 3, which shows data obtained over the frequency and amplitude ranges $0.222 \leq \omega \leq 24.4$, and $0.5 < \Delta \leq 1$, together with the effective thresholds derived from integration of the inhomogeneous Eqs. (1) with $f=0.0004$. At each ω the value of Δ matches that of the experiment and the theoretical points are connected by a dashed line as a guide to the eye. Also included in the plot are results derived from the amplitude criterion of RH with $M=2.25$, similarly matched in Δ . Both methods of parametrizing the problem appear to provide a good qualitative description of our results, with only a few exceptions.

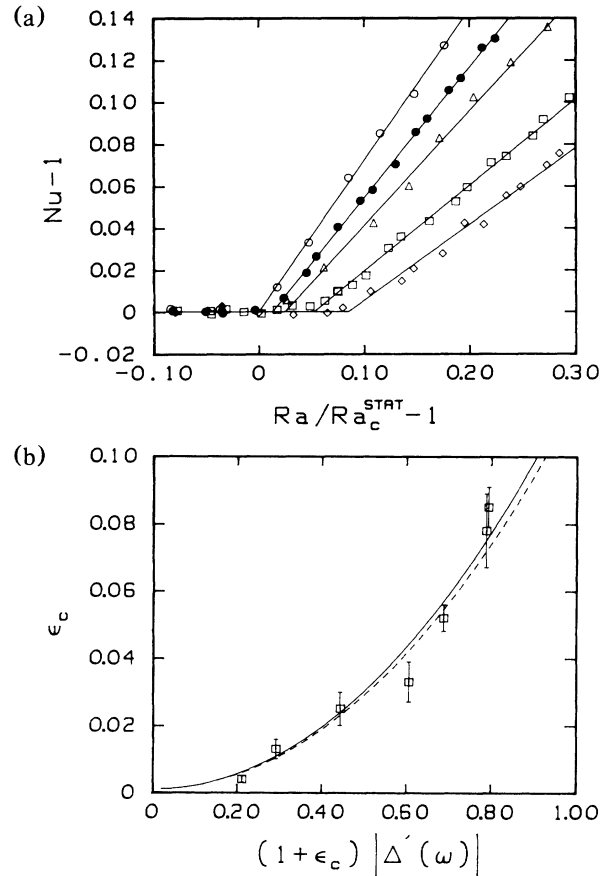


FIG. 2. Moderately high-frequency modulation: $\omega=10.7$. (a) Open circles, $\Delta=0$; filled circles, $\Delta=0.30$; triangles, $\Delta=0.45$; squares, $\Delta=0.68$; lozenges, $\Delta=0.76$. The data were obtained for a top-plate modulation. The lines represent fits to the data as in Fig. 1. (b) Convective threshold ϵ_c vs $\delta'_c = (1 + \epsilon_c) |\Delta'(\omega)|$ for $\omega=10.7$. Squares are experimental values [see (a)]. The solid line represents stability results for the ideal system [Eqs. (1)]. The dashed line is also obtained from Eqs. (1) but with forcing (1a') and a forcing strength $f=4 \times 10^{-4}$.

Finally, we mention that the apparently systematic reduction in the initial slope of the heat transfer above threshold [see Fig. 2(a)], as the relative amplitude Δ is increased, is also predicted by the model of AHL. While the qualitative trend is correct, the experimental slopes appear to be smaller than the values suggested by the model.

Further details of the experiment as well as results of modulation with two commensurate and incommensurate frequencies and with broad-band noise will be reported elsewhere.¹⁸

The authors gratefully acknowledge useful conversations concerning this experiment with Professor Guenter Ahlers and Professor Simon Rosenblat. This research was supported by the National Science Foundation Fluid

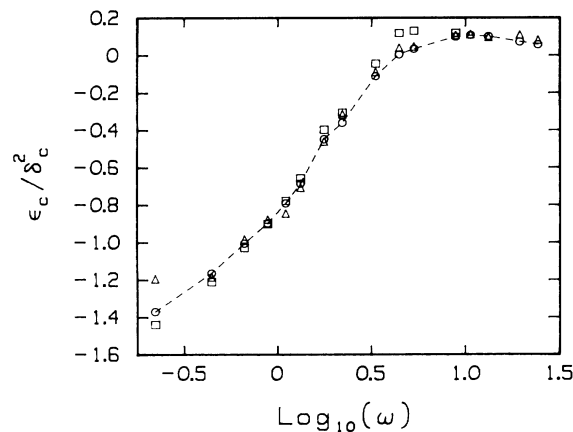


FIG. 3. ϵ_c/δ_c^2 as a function of modulation frequency for $0.5 < \Delta \leq 1$. Triangles are experimental data. Circles result from an integration of Eqs. (1) with the inhomogeneous forcing term and a forcing strength $f=4 \times 10^{-4}$. Squares represent the threshold according to the amplitude criterion [Eqs. (5.17) and (5.18) of Ref. 1 with $M=2.25$]. At each value of ω the theoretical points (circles and squares) have been calculated with use of the value of Δ corresponding to the experimental point (triangle) at that ω . The dashed line joins circles [Eqs. (1)] as a guide to the eye.

Mechanics Program under Grant No. MSM 81-17569 and the National Science Foundation Heat Transfer Program under Grant No. MEA 83-20402.

¹S. Rosenblat and D. M. Herbert, J. Fluid Mech. **43**, 385

(1969).

²S. Rosenblat and G. A. Tanaka, Phys. Fluids **14**, 1319 (1971).

³M. N. Roppo, S. H. Davis, and S. Rosenblat, Phys. Fluids **27**, 796 (1984).

⁴G. Ahlers, P. C. Hohenberg, and M. Lücke, Phys. Rev. A **32**, 3493 (1985), and references therein.

⁵P. C. Hohenberg and J. B. Swift, Phys. Rev. B **35**, 3493 (1985).

⁶J. B. Swift and P. C. Hohenberg, Phys. Rev. A (to be published).

⁷S. H. Davis, Annu. Rev. Fluid Mech. **8**, 57 (1976), and references therein.

⁸R. G. Finucane and R. E. Kelly, Int. J. Heat Mass Transfer **19**, 71 (1976).

⁹J. P. Gollub and S. V. Benson, Phys. Rev. Lett. **41**, 948 (1978).

¹⁰G. Ahlers, P. C. Hohenberg, and M. Lücke, Phys. Rev. A **32**, 3519 (1985).

¹¹J. J. Niemela and R. J. Donnelly, Phys. Rev. Lett. **57**, 583 (1986).

¹²T. Walsh, W. T. Wagner, and R. J. Donnelly, Phys. Rev. Lett. **58**, 2543 (1987).

¹³A. H. Nayfeh and D. T. Mook, *Nonlinear Oscillations* (Wiley, New York, 1979).

¹⁴L. D. Landau and E. M. Lifshitz, *Course of Theoretical Physics Mechanics* (Pergamon, New York, 1960), Vol. 1.

¹⁵E. N. Lorenz, J. Atmos. Sci. **20**, 130 (1963).

¹⁶The expression for $\Delta'(\omega)$ given by AHL [Ref. 4, Eq. (2.32e)] contains a misprint. The correct expression is

$$\Delta'(\omega) = \Delta(9\pi^4\gamma)[2 \tan \frac{1}{2} \gamma(\pi^2 - \gamma^2)(9\pi^2 - \gamma^2)]^{-1},$$

where $\gamma = (i\omega)^{1/2}$.

¹⁷R. J. Donnelly, Proc. Roy. Soc. London A **281**, 130 (1964).

¹⁸J. J. Niemela and R. J. Donnelly, unpublished.